

# Bridging Two Ways of Describing Final-State Interactions in $A(e, e'p)$ Reactions

D. Debruyne, J. Ryckebusch, S. Janssen and T. Van Cauteren

*Department of Subatomic and Radiation Physics,  
Ghent University, Proeftuinstraat 86, B-9000 Gent, Belgium*

(November 21, 2018)

We outline a relativistic and unfactorized framework to treat the final-state interactions in quasi-elastic  $A(e, e'p)$  reactions for four-momentum transfers  $Q^2 \gtrsim 0.3$  (GeV/c)<sup>2</sup>. The model, which relies on the eikonal approximation, can be used in combination with optical potentials, as well as with the Glauber multiple-scattering method. We argue that such a model can bridge the gap between a typical “low” and “high-energy” description of final-state interactions, in a reasonably smooth fashion. This argument is made on the basis of calculated structure functions, polarization observables and nuclear transparencies for the target nuclei <sup>12</sup>C and <sup>16</sup>O.

*PACS:* 24.10.-i, 24.10.Jv, 25.30.Fj

*Keywords:* Relativistic Eikonal Approximation, Glauber Theory, Exclusive  $A(e, e'p)$  Reactions, Nuclear Transparency.

## I. INTRODUCTION

At intermediate values of the four-momentum transfer, here loosely defined as  $Q^2 \geq 0.5$  (GeV/c)<sup>2</sup>, the exclusive electroinduced  $\vec{e} + A \rightarrow e' + (A - 1)^* + \vec{p}$  reaction offers great opportunities to study the properties of bound nucleons in a regime where one expects that both hadronic and partonic degrees of freedom may play a role. One such example is the study of the short-range structure of nuclei. These studies are meant to provide insight into the origin of the large-momenta components in the nucleus. Amongst other things, constituent-quark models for the nucleon predict measurable medium modifications of the bound nucleon’s properties. At present, high-resolution double polarization experiments of  $A(\vec{e}, e'\vec{p})$  reactions are putting these predictions to stringent tests [1]. Another medium-dependent effect, which has attracted a lot of attention in recent years, is the color transparency (CT) phenomenon. For  $A(e, e'p)$  processes, CT predicts that, at sufficiently high values of  $Q^2$ , the struck proton may interact in an anomalously weak manner with the spectator nucleons in the target nucleus [2].

For all of the aforementioned physics issues, the interpretation of the  $A(e, e'p)$  measurements very much depends on the availability of realistic models to describe the final-state interactions (FSI) which the ejected proton is subject to. There are basically two classes of models to treat the FSI effects in electroinduced proton knockout. At lower energies, most theoretical  $A(e, e'p)$  investigations are performed within the context of the so-called distorted-wave impulse approximation (DWIA), where the scattering wavefunction of the struck nucleon is calculated in a potential model [3]. The parameters in these optical potentials, which are available in both relativistic and non-relativistic forms, are obtained from global fits to elastic proton-nucleus scattering data. The DWIA calculations typically rely on partial-wave expansions of the exact solutions to the scattering problem, a method which becomes increasingly cumbersome at higher energies. To make matters worse, global parametrizations of optical potentials are usually not available for proton kinetic energies beyond 1 GeV. In this energy regime the Glauber model [4], which is a multiple-scattering extension of the eikonal approximation, offers a valid alternative for describing final-state interactions. In such a framework, the effects of FSI are calculated directly from the elementary proton-nucleon scattering data through the introduction of a profile function [5–9]. Several non-relativistic studies have formally investigated the applicability of the Glauber model for describing  $A(e, e'p)$  reactions at higher energies and momentum transfers. These investigations were often hampered by the lack of high-quality  $A(e, e'p)$  data to compare the model calculations with. Recently, the first high-quality data for <sup>16</sup>O( $e, e'p$ ) cross sections, separated structure functions and polarization observables at  $Q^2 = 0.8$  (GeV/c)<sup>2</sup> became available [10].

The purpose of this letter is to investigate whether the optical potential and the Glauber method for describing final-state interactions lead to comparable results in an energy regime where both methods appear applicable. An observation which may point towards inconsistencies in the description of FSI effects in  $A(e, e'p)$  processes at “low” and “high” energies, is the apparent  $Q^2$  evolution of the extracted spectroscopic factors [11]. Whereas numerous optical-potential analyses of  $A(e, e'p)$  measurements at low  $Q^2$  have systematically produced values which represent 50-70% of the sum-rule strength, it has recently been suggested that in order to describe the data at higher  $Q^2$  within the context of the Glauber model, substantially higher values are required [11,12].

We propose a relativistic formalism for computing  $A(e, e'p)$  observables at medium energies. The formalism is developed in such a way that it can be used in combination with either optical potentials or the Glauber method without affecting any other ingredient of the model. Results of optical potential and Glauber like calculations of

structure functions and polarization observables for the target nuclei  $^{16}\text{O}$  and  $^{12}\text{C}$  are presented and compared. In addition, results of relativistic and unfactorized nuclear transparency calculations for the  $^{12}\text{C}(e, e'p)$  reaction are presented.

## II. FORMALISM

In the one-photon-exchange approximation, the cross section for a process in which an electron impinges on a nucleus and induces the knockout of a single nucleon with momentum  $k_f$ , leaving the residual nucleus in a certain discrete state, can be written in the following form [13]

$$\left( \frac{d^5\sigma}{d\epsilon' d\Omega_{e'} d\Omega_f} \right) = \frac{M_p M_{A-1} k_f}{8\pi^3 M_A} f_{rec}^{-1} \sigma_M \left[ v_L \mathcal{R}_L + v_T \mathcal{R}_T + v_{TT} \mathcal{R}_{TT} + v_{TL} \mathcal{R}_{TL} \right], \quad (1)$$

where  $f_{rec}$  is the hadronic recoil factor, and  $\sigma_M$  is the Mott cross section. The electron kinematical factors  $v_i$  and the structure functions  $R_i$  are defined in the usual manner [13]. Remark that in our model calculations an unfactorized expression for the differential cross section is adopted. This means that the off-shell electron-proton coupling is not separated from the nuclear dynamics. Although the factorized approach has long been abandoned in the description of low-energy  $A(e, e'p)$  reactions, it is still widely used when it comes to describing high-energy  $A(e, e'p)$  processes.

In our model, the relativistic bound-state wavefunctions are calculated within the context of a mean-field approximation to the  $\sigma - \omega$  model [14,15]. Assuming spherical symmetry, the following type of solutions to the Dirac eigenvalue problem result

$$\psi_\alpha(\vec{r}) \equiv \psi_{n\kappa m t}(\vec{r}) = \begin{bmatrix} iG_{n\kappa t}(r)/r \mathcal{Y}_{\kappa m} \eta_t \\ -F_{n\kappa t}(r)/r \mathcal{Y}_{-\kappa m} \eta_t \end{bmatrix}, \quad (2)$$

where  $n$  denotes the principal,  $\kappa$  and  $m$  the generalized angular momentum and  $t$  the isospin quantum numbers. The  $\mathcal{Y}_{\pm\kappa m}$  are the well-known spin-spherical harmonics and determine the angular and spin parts of the wavefunction. In solving the relativistic bound-state problem, we have adopted the values for the coupling constants and meson masses of Ref. [15].

In the relativistic eikonal approximation, the scattering wave function for a nucleon subject to a scalar ( $V_s$ ) and a vector potential ( $V_v$ ) reads

$$\psi_{\vec{k}_f, s}^{(+)} = \sqrt{\frac{E+M}{2M}} \left[ \frac{1}{E+M+V_s-V_v} \vec{\sigma} \cdot \vec{p} \right] e^{i\vec{k}_f \cdot \vec{r}} e^{iS(\vec{r})} \chi_{\frac{1}{2}m_s}, \quad (3)$$

where the eikonal phase  $S(\vec{b}, z)$  is defined as

$$iS(\vec{b}, z) = -i \frac{M}{K} \int_{-\infty}^z dz' \left[ V_c(\vec{b}, z') + V_{so}(\vec{b}, z') \left[ \vec{\sigma} \cdot (\vec{b} \times \vec{K}) - iKz' \right] \right], \quad (4)$$

with  $\vec{r} \equiv (\vec{b}, z)$  and  $\vec{K} \equiv \frac{1}{2}(\vec{q} + \vec{k}_f)$ . The central  $V_c$  and spin-orbit potential  $V_{so}$  occurring in the above expression are determined by  $V_s$  and  $V_v$  and their derivatives. In general, strength from the incident beam is drained into other inelastic channels. Within the context of a DWIA approach, the inelasticities are commonly implemented through the use of a complex optical potential which is gauged against elastic  $pA$  scattering data. In the numerical calculations, we have used the global relativistic optical potentials of Cooper et al. [16]. By fitting proton elastic scattering data in the energy range of 20 - 1040 MeV, Cooper *et al.* obtained a set of energy-dependent potentials for the target nuclei  $^{12}\text{C}$ ,  $^{16}\text{O}$ ,  $^{40}\text{Ca}$ ,  $^{90}\text{Zr}$  and  $^{208}\text{Pb}$ . In what follows, we refer to calculations on the basis of Eq. (3) as the optical model eikonal approximation (OMEA).

For proton kinetic energies  $T_p \geq 1$  GeV, the use of optical potentials appears no longer justifiable in view of the highly inelastic character of the elementary proton-nucleon scattering process. Here, a way out is offered by an extension of the eikonal method, namely the Glauber multiple-scattering method, which is usually adopted in its non-relativistic version. Here, we propose the use of a relativized version which allows us to write the wavefunction of the escaping proton as

$$\psi_{\vec{k}_f, s}^{(+)} = \sqrt{\frac{E+M}{2M}} \hat{S} \left[ \frac{1}{E+M} \vec{\sigma} \cdot \vec{p} \right] e^{i\vec{k}_f \cdot \vec{r}} \chi_{\frac{1}{2}m_s}. \quad (5)$$

This expression for the relativistic scattering wave function is derived in similar manner as for the non-relativistic (NR) case where the wave function adopts the well-known form

$$\psi_{\vec{k}_f, s}^{(+), NR} = \hat{S} e^{i\vec{k}_f \cdot \vec{r}} \chi_{\frac{1}{2}m_s} . \quad (6)$$

The operator  $\hat{S}$  defines the action of the subsequent collisions that the ejectile undergoes with the spectator nucleons

$$\hat{S}(\vec{r}, \vec{r}_2, \dots, \vec{r}_A) = \prod_{j=2}^A \left[ 1 - \Gamma(\vec{b} - \vec{b}_j) \theta(z - z_j) \right] , \quad (7)$$

where  $\theta(z - z_j)$  ensures that the hit proton only interacts with other nucleons if they are localised in its forward propagation path. The profile function  $\Gamma(k_f, \vec{b})$  for central elastic pN scattering reads

$$\Gamma(k_f, \vec{b}) = \frac{\sigma_{pN}^{tot} (1 - i\epsilon_{pN})}{4\pi\beta_{pN}^2} \exp\left(-\frac{b^2}{2\beta_{pN}^2}\right) . \quad (8)$$

The parameters in Eq. (8) can be taken directly from nucleon-nucleon scattering measurements and include the total pN cross sections  $\sigma_{pN}^{tot}$ , the slope parameters  $\beta_{pN}$  and the ratios of the real to imaginary part of the scattering amplitude  $\epsilon_{pN}$ . The  $A(e, e'p)$  calculations on the basis of the scattering state of Eq. (5) are hereafter referred to as the relativistic multiple-scattering Glauber approximation (RMSGGA).

### III. RESULTS

We first compare our relativistic calculations to recent quasi-elastic  $^{16}\text{O}(e, e'p)$  data from JLAB. In these high-resolution experiments at  $Q^2 = 0.8$  (GeV/c)<sup>2</sup> differential cross sections, separated structure functions and polarization observables were obtained [10]. The variation in missing momentum was achieved by varying the detection angle of the ejected proton with respect to the direction of the momentum transfer (“quasi-perpendicular kinematics”). Hence, it was only possible to isolate the combination  $R_{L+TT} \equiv R_L + \frac{v_{TT}}{v_L} R_{TT}$ . In Fig. 1 we display the different structure functions against the missing momentum  $p_m$ . The different curves all use the same bound-state wavefunctions and electron-proton coupling but differ in the way the FSI are treated. In Table I we display the spectroscopic factors which are obtained from a  $\chi^2$  fit from the calculations to the data. Although the Glauber and the optical-potential framework provide an intrinsically very different treatment of the final-state interactions, they lead to almost identical spectroscopic factors at  $Q^2 = 0.8$  (GeV/c)<sup>2</sup>. Another striking observation from Fig. 1 is that both types of calculations produce almost identical results for the  $R_T$  and  $R_{L+TT}$  structure functions. In the  $R_{TL}$  response for excitation of the 6.3 MeV  $\frac{3}{2}^-$  state the differences are somewhat larger. It is worth mentioning here that of all structure functions, the  $R_{TL}$  one has been identified as being most sensitive to changes in the current operator and relativistic corrections [17–19].

A quantity which is particularly sensitive to FSI effects is the induced polarization  $P_n$

$$P_n = \frac{\sigma(s_N^i = \uparrow) - \sigma(s_N^i = \downarrow)}{\sigma(s_N^i = \uparrow) + \sigma(s_N^i = \downarrow)} , \quad (9)$$

where  $s_N^i$  denotes the spin orientation of the ejectile in the direction orthogonal to the reaction plane. In the  $^{12}\text{C}(e, e'\vec{p})$  experiment of Woo and collaborators [21], the quantity  $P_n$  was determined at quasifree kinematics for an energy and momentum transfer of  $(\omega, q) = (294 \text{ MeV}, 756 \text{ MeV}/c)$ . The results of the  $^{12}\text{C}(e, e'\vec{p})$  measurements are shown in Fig. 2, along with our theoretical results. The fair agreement of the Glauber results with the data is striking. It turns out that the applicability of the RMSGGA method is wider than one would naively expect. We believe that the extended range of validity of the RMSGGA method observed here, is (partly) caused by the relativistic and unfactorized treatment of the Glauber method. In Ref. [22] we have demonstrated that the effect of dynamical relativity (i.e. the effect of the lower components of the wavefunctions) can be significant at low  $Q^2$ .

We now turn to the study of the nuclear transparency in the quasi-elastic  $^{12}\text{C}(e, e'p)$  reaction in a wide  $Q^2$  range of  $0.3 \leq Q^2 \leq 20$  (GeV/c)<sup>2</sup>. The results of our calculations are contained in Fig. 3. We have performed calculations within the relativistic Glauber framework and the eikonal model with the optical potentials from Ref. [16]. The optical potential results are limited to kinetic energies below  $T_p = 1$  GeV. In the Glauber model, we have also performed calculations which include the effect of short-range correlations (SRC). Each of these calculations was done

with the CC1 and CC2 current operator. The transparencies calculated within the Glauber framework exhibit some fluctuations. The magnitude of these fluctuations mark the intrinsic uncertainties on the computed transparencies caused by the error bars on the measured elementary pN scattering parameters. Most published Glauber calculations for the nuclear transparencies do not exhibit these fluctuations, but use (smooth) global fits to determine the energy dependence of the elementary pN scattering data. In our numerical calculations, we use the listed experimental pN results.

The measurements in Refs. [23–25] were performed in certain regions of the phase space, dictated by the requirement that quasi-elastic conditions should be met. We have constrained our calculations to the same segment of the phase space. In general, the experimental transparency  $T_{exp}$  is defined as

$$T_{exp} = \frac{\int_{\Delta^3 k} d\vec{k} \int_{\Delta E} dE \left( \frac{d^5 \sigma}{d\epsilon' d\Omega_{e'} d\Omega_f} \right)_{exp}}{c_A \int_{\Delta^3 k} \int_{\Delta E} dE \left( \frac{d^5 \sigma}{d\epsilon' d\Omega_{e'} d\Omega_f} \right)_{PWIA}}. \quad (10)$$

The A-dependent factor  $c_A$  renormalizes the non-relativistic plane-wave impulse approximation (PWIA) predictions for corrections induced by SRC. For the  $^{12}\text{C}(e, e'p)$  process, a correction factor of  $0.901 \pm 0.024$  was adopted in Refs. [23–25]. As the implementation of short-range correlations can be done in numerous ways, we have removed this factor and rescaled the data accordingly.

At lower values of  $Q^2$  there are substantial deviations between the transparencies computed with the CC1 and the CC2 current operator. At higher values of  $Q^2$  [ $Q^2 \geq 3 - 4$  (GeV/c) $^2$ ], where the differences between the CC1 and CC2 predictions are negligible, the predicted transparencies tend to underestimate the measured transparencies, even when assuming full occupancy for the single-particle levels in  $^{12}\text{C}$ . This apparent shortcoming can be cured by introducing the effect of short-range correlations. They are implemented through the introduction of a central (or, Jastrow) correlation function  $g(|\vec{r}_1 - \vec{r}_2|)$  in the two-body density components which are part of the Glauber calculations. In practice, this procedure amounts to the following replacement in the matrix elements that determine the rescattering effects

$$\psi_\alpha(\vec{r}_1) \psi_\beta(\vec{r}_2) \longrightarrow \psi_\alpha(\vec{r}_1) \psi_\beta(\vec{r}_2) g(|\vec{r}_1 - \vec{r}_2|). \quad (11)$$

In line with the findings of other studies [6,12,26,27,29] we observe that short-range correlations increase the calculated transparencies by about 10 %. We have used the central correlation function  $g_{GD}(r)$  from a nuclear-matter calculation of Gearhart and Dickhoff [30]. Amongst different other candidates, this correlation function emerged as the preferred choice in an analysis of  $^{12}\text{C}(e, e'pp)$  data [31]. Being a rather hard correlation function, the effect of introducing  $g_{GD}(r)$  on the computed values of the transparencies is maximized. We have also evaluated the role of relativistic effects on the computed transparencies. In general, these effects are rather small. For example, the coupling between the lower component in the bound and scattering state marginally affects the predictions for the transparencies. For some specific observables, like the  $R_{TL}$  structure function in Fig. 1, on the other hand, the relativistic effects are substantial.

For four-momentum transfers about  $Q^2 \approx 1$  (GeV/c) $^2$  it appears legitimate to directly compare the optical potential and the Glauber calculations. It is obvious from Fig. 3 that the OMEA curves exhibit a behaviour very similar to the correlated Glauber results. This observation may suggest that the in-medium pN cross sections are modestly reduced compared to the on-shell values and that the major part of this effect can be modeled through the introduction of SRC mechanisms. As for the OMEA results, it can be argued that the SRC effects, which belong to the class of medium effects, are already effectively incorporated in the formalism. After all, the optical potentials are obtained from a global fit to proton-nucleus scattering data.

The apparent consistency between the OMEA and the correlated RMSGA predictions is an interesting result. Indeed, it demonstrates that the low and the high  $Q^2$  regime can be bridged in a satisfactory manner. This feature has its consequences for the apparent  $Q^2$  evolution of the spectroscopic factors extracted from  $^{12}\text{C}(e, e'p)$  [11]. As suggested by the authors of Ref. [11], a consistent analysis of all  $^{12}\text{C}(e, e'p)$  data between  $0.1 \leq Q^2 \leq 10$  (GeV/c) $^2$  could much improve insight into this matter. A consistent treatment would at least allow to separate genuine physical effects (contributions from meson exchange,  $\Delta$ -isobars, SRC etc.) from model-dependent uncertainties (like gauge ambiguities and problems related to the treatment of the FSI). Such an analysis should preferably be carried out in a framework that is able to describe both the low and high  $Q^2$  ( $e, e'p$ ) data without any inconsistencies in some intermediate-energy range. We feel that the framework presented here, is an initial step in this direction.

## IV. CONCLUSION

Summarizing, we have outlined a relativistic and unfactorized framework for computing  $A(e, e'p)$  observables at intermediate and high four-momentum transfers  $Q^2$ . The model is based on the eikonal approximation and can accommodate both relativistic optical potentials and a Glauber approach, which are two substantially different techniques to deal with final-state interactions. We have shown that optical-potential and Glauber predictions are reasonably consistent at intermediate values of  $Q^2$ . Indeed, at  $Q^2$  values of about  $0.8 \text{ (GeV/c)}^2$ , which is a regime in which both approaches for dealing with the FSI's appear justified, comparable results for the transparencies and structure functions are obtained.

- [1] S. Dieterich *et al.*, Phys. Lett. **B500** (2001) 47.
- [2] L. Frankfurt, G. Miller and M. Strikman, Annu. Rev. Nucl. Part. Sci. **45** (1994) 501.
- [3] A. Picklesimer, J. Van Orden and S. Wallace, Phys. Rev. **C32** (1985) 1312.
- [4] R. Glauber and G. Matthiae, Nucl. Phys. **B21** (1970) 135.
- [5] S. Jeschonnek and T. Donnelly, Phys. Rev. C **59** (1999) 2676.
- [6] L. Frankfurt, E. Moniz, M. Sargsyan and M. Strikman, Phys. Rev. C **51** (1995) 3435.
- [7] O. Benhar, S. Fantoni, N. Nikolaev, J. Speth, A. Usmani and B. Zakharov, Z. Phys. **A355** (1996) 267.
- [8] N. Nikolaev, A. Szcurek, J. Speth, J. Wambach, B. Zakharov and V. Zoller, Nucl. Phys. **A582** (1995) 665.
- [9] C. Ciofi degli Atti and D. Treleani, Phys. Rev. C **60** (1999) 024602.
- [10] J. Gao *et al.*, Phys. Rev. Lett. **84** (2000) 3265.
- [11] L. Lapikas, G. van der Steenhoven, L. Frankfurt, M. Strikman and M. Zhalov, Phys. Rev. C **61** (2000) 064325.
- [12] L. Frankfurt, M. Strikman and M. Zhalov, Phys. Lett. **B503** (2001) 73.
- [13] A. Raskin and T. Donnelly, Adv. Nucl. Phys. **191** (1989) 78.
- [14] C. Horowitz and B. Serot, Nucl. Phys. A **368** (1981) 503.
- [15] B. Serot and J. Walecka, Adv. Nucl. Phys. **16** (1986) 1.
- [16] E. Cooper, S. Hama, B. Clarck and R. Mercer, Phys. Rev. C **47** (1993) 297.
- [17] J. Udias, J. Caballero, E. Moya de Guerra, J. Amaro and T. Donnelly, Phys. Rev. Lett. **83** (1999) 5451.
- [18] S. Gardner and J. Piekarewicz, Phys. Rev. C **50** (1994) 2822.
- [19] S. Jeschonnek and T. Donnelly, Phys. Rev. C **57** (1998) 2438.
- [20] J. Udias and J. Vignote, Phys. Rev. C **62** (2000) 034302.
- [21] R. Woo *et al.*, Phys. Rev. Lett. **80** (1998) 456.
- [22] D. Debruyne, J. Ryckebusch, W. Van Nespén and S. Janssen, Phys. Rev. C **62** (2000) 024611.
- [23] N. Makins *et al.*, Phys. Rev. Lett. **72** (1994) 1986.
- [24] T. O'Neill *et al.*, Phys. Lett. **B351** (1995) 87.
- [25] D. Abbott *et al.*, Phys. Rev. Lett. **80** (1998) 5072.
- [26] A. Kohama, K. Yazaki and R. Seki, Nucl. Phys. **A551** (1993) 687.
- [27] O. Benhar, A. Fabrocini, S. Fantoni, V. Pandharipande and I. Sick, Phys. Rev. Lett. **69** (1992) 881.
- [28] R. Seki, T. Shoppa, A. Kohama and K. Yazaki, Phys. Lett. **B383** (1996) 133.
- [29] V. Pandharipande and S. Pieper, Phys. Rev. C **45** (1992) 791.
- [30] C. Gearheart, PhD thesis, unpublished, Washington University, St. Louis, (1994).
- [31] K. Blomqvist *et al.*, Phys. Lett. **B421** (1998) 71.
- [32] G. Garino *et al.*, Phys. Rev. **C45** (1992) 780.

	CC1 operator			CC2 operator		
	<i>RPWIA</i>	<i>OMEA</i>	<i>RMSGa</i>	<i>RPWIA</i>	<i>OMEA</i>	<i>RMSGa</i>
$\frac{3}{2}^- (E_x=6.3 \text{ MeV})$	0.59	0.96	0.96	0.61	1.00	1.00
$\frac{1}{2}^- (\text{g.s.})$	0.53	0.79	0.80	0.53	0.82	0.82

TABLE I. The spectroscopic factors as derived from the  $^{16}\text{O}(e, e'p)$  results contained in Fig. 1 through a  $\chi^2$  fitting procedure.

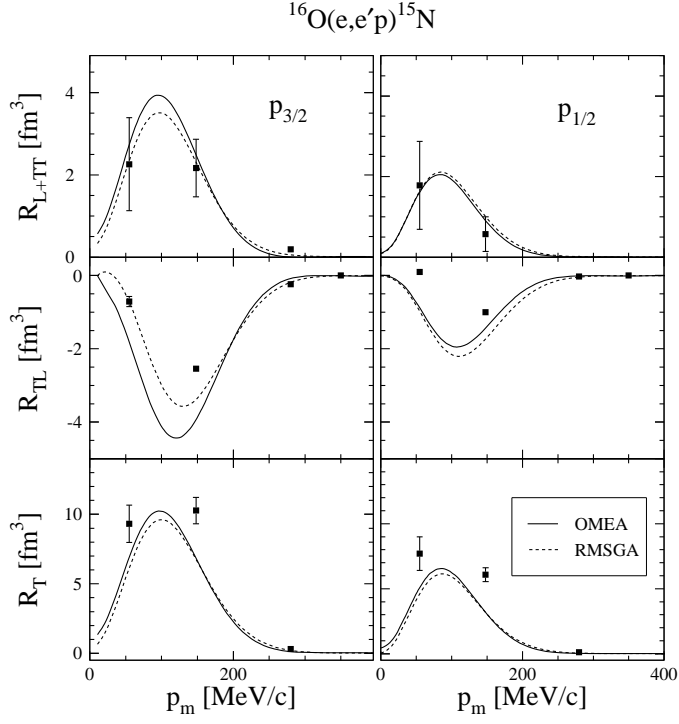


FIG. 1. Separated structure functions for  $^{16}\text{O}(e,e'p)^{15}\text{N}$  in quasi-perpendicular kinematics at  $\epsilon=2.4$  GeV,  $q=1$  GeV/c and  $\omega=0.439$  GeV. The solid and dashed curves denote the eikonal (OMEA) and Glauber (RMSGa) calculations. The data are from Ref. [10].

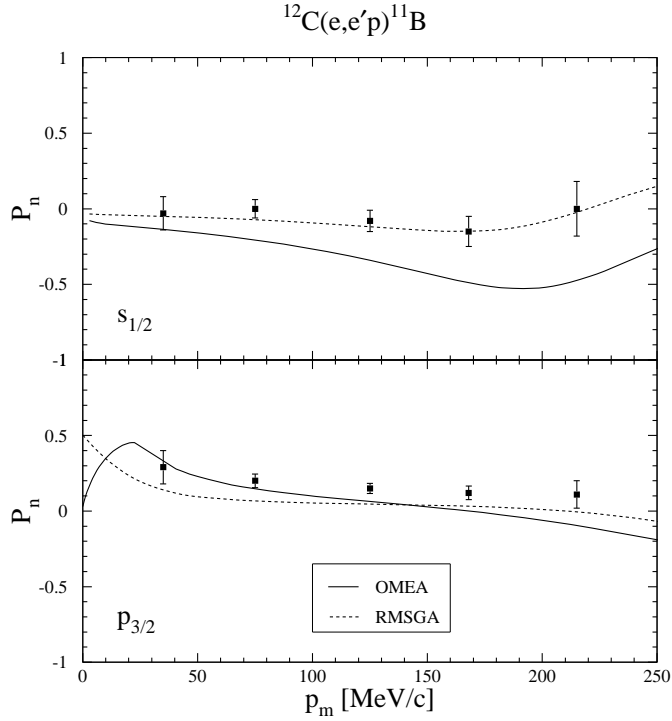


FIG. 2. Induced polarization for the  $^{12}\text{C}(e, e'p)^{11}\text{B}$  reaction in quasi-perpendicular kinematics at  $\epsilon=579$  MeV,  $q=756$  MeV/c and  $\omega=294$  MeV. The data are from Ref. [21].

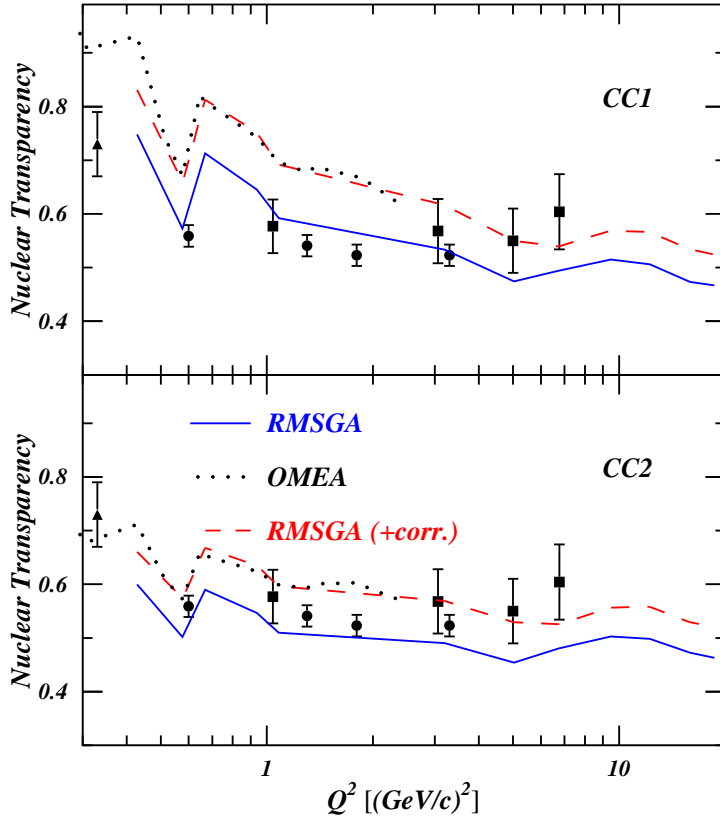


FIG. 3. Nuclear transparency for  $^{12}\text{C}(e, e'p)$  as a function of  $Q^2$ . The curves denote calculations within the relativistic Glauber framework (RMSGGA) and the eikonal model with optical potentials (OMEA). Glauber results with and without inclusion of SRC effects are presented. The calculations in the upper (lower) panel employ the CC1 (CC2) current operator. The curves assume full occupancy of the  $s$  and  $p$ -shell levels in  $^{12}\text{C}$ . The data are from BATES [32] (triangles), SLAC [23,24] (squares) and from JLAB [25] (circles).